Int. J. Solids Structures Vol. 26, No. 8, pp. 865–886, 1990
Printed in Great Britain.

0020-7683/90 $3.00 + .00

CRITICAL INITIAL IMPERFECTION OF STRUCTURES

KIYOHIRO IKEDA
Department of Civil Engineering, Nagaoka University of Technology, Nagaoka, Niigata 940-21, Japan

and

KAZUO MUROTA
Department of Civil Engineering, Nagaoka University of Technology, Nagaoka, Niigata 940-21,

(*Received* 28 *March* 1989; *in revised form* 19 *September* 1989)

Abstract—A method is introduced for determining the critical initial imperfection of discretized structures that decreases the load-bearing capacity most rapidly. The effects of imperfections on simple critical points, such as limit points of loads and simple bifurcation points, are theoretically investigated based on the idea of the Lyapunov–Schmidt decomposition developed in bifurcation theory. Imperfection sensitivity varies with the types of points. Nonetheless critical imperfection pattern is expressed in the same formula regardless of the types. Among various imperfections, the most influential can be found in a quantitative manner. The validity and the usability of the proposed method are illustrated through its application to simple example structures.

1. INTRODUCTION

The load-bearing capacity of a real structure is highly sensitive to imperfections to which the members and materials are all subjected. This is particularly the case for structures undergoing bifurcation buckling, such as domes and shells (Hutchinson and Koiter, 1970). In the design of such structures, it is preferable to consider the "worst" imperfection that reduces the load-bearing capacity most rapidly.

Various techniques have been proposed to determine such critical imperfections. Thompson and Hunt (1973) obtained the imperfection sensitivity of a multi-degree-of-freedom system with a single imperfection parameter by applying the perturbation to the total potential energy function of the system. Hunt (1977) and Niwa *et al.* (1981) combined this approach with the catastrophe theory to determine imperfection sensitivity. Elishakoff (1988) chose initial imperfections of shells with known probabilistic properties, and Lindberg (1988) chose imperfections of the structures subjected to dynamic pulse buckling based on white noise; their critical loads for these imperfections are determined through numerical and/or experimental studies. Conbescure (1986) used the eigenmode obtained from elastic bifurcation analysis as the worst imperfection, based on the relevant observation that the eigenmode was well known to be the imperfection which would increase most rapidly.

Determining such a critical imperfection, however, remains open despite these works. Nishino and Hartono (1989) stated, "all previous works on the effect of imperfection dealt mostly with the effect of a given mode of imperfection", referring to, e.g., Rosen and Schmit (1979) and Kam and Lee (1986). Conventionally, imperfections have been selected mainly on a trial-and-error basis with one's experience and engineering sense. The lack of a method for determining the most undesirable imperfection has prevented the accurate evaluation of load-bearing capacities of dome and shell structures.

In order to address this problem, the authors introduce in this paper a method for determining the worst imperfection of elastic discretized structures that is applicable to non-degenerate simple critical points. The load-bearing capacity of an elastic structure is governed by critical points on load versus displacement relationships (equilibrium paths) which are obtained by solving the geometrically non-linear equilibrium equations. For realistic structures, these equations involve a large number of variables and are quite

complex so that a direct implementation of imperfections in general is difficult. However, by means of the Lyapunov–Schmidt decomposition in bifurcation theory (see, e.g., Sattinger, 1979; Golubitsky and Schaeffer, 1985), the complex equations are decomposed into a small number of bifurcation equations and the remaining equations; if a solution to the former is obtained, the other equations can be solved uniquely by the implicit function theorem. In particular, in the neighborhood of a simple critical point, equilibrium equations reduce to a single bifurcation equation. The critical imperfection is to be determined from the bifurcation equation so that the load-bearing capacity decreases most rapidly.

The method proposed is employed to evaluate the influence of imperfections on simple example structures in order to assess its validity and applicability. The worst imperfection pattern and imperfection sensitivity are determined in the neighborhood of various kinds of simple critical points, including: the limit (stationary) point of the loading parameter, asymmetric bifurcation point, and stable- and unstable-symmetric bifurcation points. A suggestion toward future studies concludes this paper.

2. AN ILLUSTRATIVE EXAMPLE

Before presenting the general theory in Section 3, we will demonstrate our general approach by using a simple example. Consider the non-shallow truss arch in Fig. 1, whose load-bearing capacity is governed by an unstable-symmetric bifurcation point A as in Fig. 2.

The equilibrium under a vertical load f is described by

$$f\begin{pmatrix}0\\1\end{pmatrix}=\begin{pmatrix}F_x\\F_y\end{pmatrix}=\begin{bmatrix}\sum_{i=1}^{2} EA_i(1/L_i-1/\hat{L}_i)(x-x_i)\\ \sum_{i=1}^{2} EA_i(1/L_i-1/\hat{L}_i)(y-y_i)\end{bmatrix}, \tag{1}$$

where

$$L_i=\{(x_3-x_i)^2+(y_3-y_i)^2\}^{1/2},\quad \hat{L}_i=\{(x-x_i)^2+(y-y_i)^2\}^{1/2},\quad i=1,2,$$

and EA_i expresses the product of Young's modulus and the cross-sectional area of the ith member ($i=1,2$); (x_i,y_i) is the initial location of the ith node ($i=1,2,3$); and (x,y) the location of node 3 after displacement. By solving eqn (1), we have obtained the load versus displacement curves (equilibrium paths) drawn in solid lines in Fig. 2. The bifurcation point A gives the load-bearing capacity $f_c^0=0.24776EA$ at $(x_c^0,y_c^0)=(0,0.44735)$.

Suppose that we are interested in the change $\hat{f}_c=f_c-f_c^0$ of the load-bearing capacity f_c due to small imperfections (i.e. discrepancies from the nominal values given in Fig. 1) of (x_i,y_i) $(i=1,2,3)$ and EA_i $(i=1,2)$.

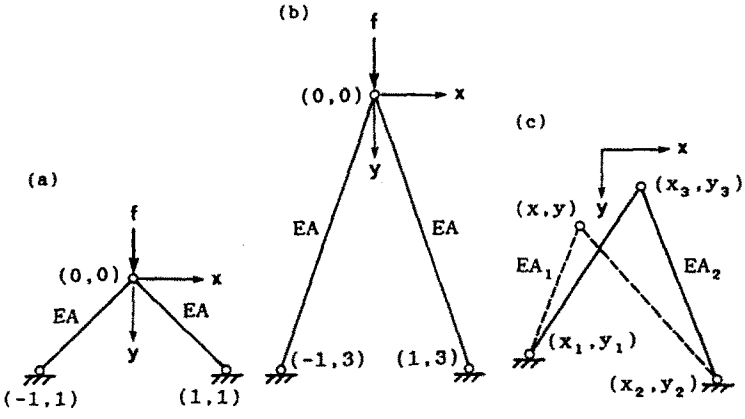

Fig. 1. Two-bar truss arches. (a) Shallow arch, (b) non-shallow arch, (c) imperfect arch.

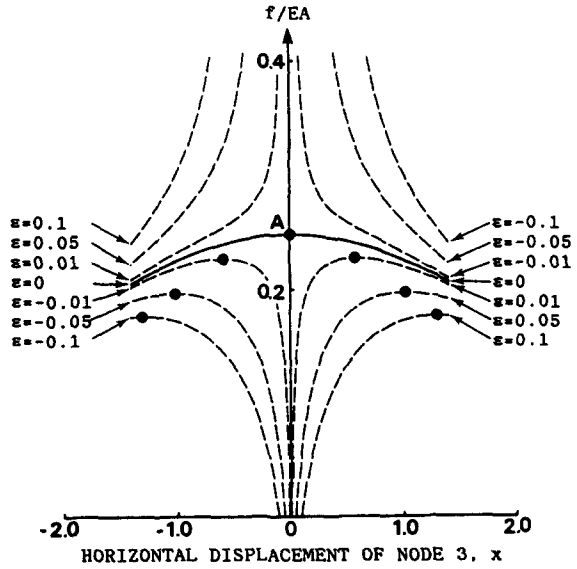

Fig. 2. f versus x curves of the non-shallow arch (unstable-symmetric bifurcation point).

If we introduce the imperfection parameter vector

$$\mathbf{v} = (x_1, y_1, x_2, y_2, x_3, y_3, EA_1, EA_2)^T,$$

we have $\mathbf{v} = \mathbf{v}^0 = (-1, 3, 1, 3, 0, 0, EA, EA)^T$ for the "perfect" system shown in Fig. 1, where $(\cdot)^T$ means the transpose of a vector. Let us further write $\mathbf{v}$ as

$$\mathbf{v} = \mathbf{v}^0 + \varepsilon \mathbf{d},$$

to distinguish the direction $\mathbf{d}$ and the magnitude $|\varepsilon|$ of an imperfection.

For a fixed direction, say,

$$\mathbf{d} = (-0.73685, -0.67606, -0.73685, 0.67606, 1, 0, EA, -EA)^T, \tag{2}$$

and various small values of $|\varepsilon|$, we have computed the equilibrium paths (indicated by broken lines in Fig. 2). Thus when $\mathbf{d}$ is kept fixed, the load-bearing capacity f_c is determined by ε. It is known as the two-thirds power law for unstable bifurcation points (see, e.g., Koiter, 1945; Thompson and Hunt, 1973) that, when ε is small,

$$\hat{f}_c \approx -C(\mathbf{d})\varepsilon^{2/3} \tag{3}$$

with a non-negative coefficient $C(\mathbf{d})$ depending on $\mathbf{d}$.

Our main concern in this paper is to determine the worst direction of the imperfection vector which causes the maximum change (decrease) of the load-bearing capacity. To be more precise, we may formulate this problem as follows. First we assume that the imperfection direction vector $\mathbf{d}$ is to be normalized as

$$\mathbf{d}^T W \mathbf{d} = 1 \tag{4}$$

with respect to a weight matrix W. In the present example we may choose, e.g.,

$$W = \text{diag}\,(1, 1, 1, 1, 1, 1, 1/(EA)^2, 1/(EA)^2). \tag{5}$$

Then our problem is to find such $\mathbf{d}$ that maximizes the coefficient $C(\mathbf{d})$ in eqn (3).

In the rest of this section we will briefly illustrate our method of analysis using this example. The reader may also proceed first to the general theory in the next section and return occasionally to this illustration.

The tangent-stiffness matrix is given by

$$J = \begin{pmatrix} J_{xx} & J_{xy} \\ J_{yx} & J_{yy} \end{pmatrix}, \tag{6}$$

where

$$J_{xx} = \sum_{i=1}^{2} EA_i\{1/L_i - (y-y_i)^2/\hat{L}_i^3\};$$

$$J_{yy} = \sum_{i=1}^{2} EA_i\{1/L_i - (x-x_i)^2/\hat{L}_i^3\};$$

$$J_{xy} = J_{yx} = \sum_{i=1}^{2} EA_i(y-y_i)(x-x_i)/\hat{L}_i^3.$$

The critical point (f_c, x_c, y_c) is determined by eqn (1) and

$$\det J = 0.$$

At the bifurcation point A, where $(f_c, x_c, y_c) = (f_c^0, x_c^0, y_c^0)$, the tangent-stiffness matrix J is singular with rank $J = 1$.

To investigate the local properties of eqn (1) around A, we consider the increment from the critical points as

$$(f, x, y) = (f_c^0 + \hat{f}, x_c^0 + w, y_c^0 + w_2). \tag{7}$$

Since $J_{yy} \neq 0$ at point A, the second equation, $F_y = f$, in eqn (1) can be solved for w_2 (i.e. for y) by the implicit function theorem as

$$w_2 = w_2(\hat{f}, w, \mathbf{v}). \tag{8}$$

On substituting eqns (7) and (8) into the first equation, $F_x = 0$, in eqn (1), we obtain a single equation

$$G(\hat{f}, w, \mathbf{v}) = \sum_{i=1}^{2} EA_i(1/L_i - 1/\hat{L}_i)(x_c^0 + w - x_i) = 0, \tag{9}$$

where

$$\hat{L}_i = \{(x_c^0 + w - x_i)^2 + (y_c^0 + w_2(\hat{f}, w, \mathbf{v}) - y_i)^2\}^{1/2}, \quad i = 1, 2.$$

Thus the original eqns (1) have reduced to a *single* equation that is much easier to handle. Such a reduction can be achieved even if the original equations have a large number of degrees of freedom, to be explained in the next section as the Lyapunov–Schmidt decomposition.

Regarding the imperfection magnitude ε as an independent variable, we put

$$\bar{G}(\hat{f}, w, \varepsilon) = G(\hat{f}, w, \mathbf{v}^0 + \varepsilon \mathbf{d}).$$

In the Taylor expansion of $\bar{G}$ around $(\hat{f}, w, \varepsilon) = (0, 0, 0)$:

$$\bar{G}(\hat{f}, w, \varepsilon) = \sum_{i=0} \sum_{j=0} \sum_{k=0} A_{ijk} w^i \hat{f}^j \varepsilon^k,$$

some of the lower order terms vanish. In fact,

$$A_{000} = \bar{G}(0,0,0) = 0. \quad A_{100} = \partial\bar{G}(0,0,0)/\partial w = 0 \tag{10}$$

since $(\hat{f}, w, \varepsilon) = (0,0,0)$ corresponds to the critical point for the perfect system. We also see

$$A_{010} = 0, \quad A_{200} = 0, \quad A_{300} \neq 0, \quad A_{110} \neq 0. \tag{11}$$

The lowest order term in ε, which governs the imperfection sensitivity as we will see later, is computed from eqn (9) as

$$A_{001} = \partial\bar{G}/\partial\varepsilon = (\partial G/\partial \mathbf{v})\,\mathbf{d}, \tag{12}$$

where in our example,

$$\partial G/\partial \mathbf{v} = EA(0.03162, 0.02901, 0.03162, -0.02901, -0.06325, 0, -0.04853/EA, 0.04853/EA)^{\mathrm{T}}. \tag{13}$$

The following three-term approximation turns out to be sufficient for our purpose:

$$\bar{G} \approx A_{300}w^3 + A_{110}\hat{f}w + A_{001}\varepsilon, \tag{14}$$

from which we obtain

$$\partial\bar{G}/\partial w \approx 3A_{300}w^2 + A_{110}\hat{f}. \tag{15}$$

The critical point $(\hat{f}_c, w)$ of the imperfect system is determined by

$$\bar{G} = 0, \quad \partial\bar{G}/\partial w = 0. \tag{16}$$

On substituting eqns (14) and (15) into eqn (16) and eliminating w, we obtain eqn (3) with

$$C(\mathbf{d}) = \frac{3}{|A_{110}|}|A_{300}|^{1/3}\left|\frac{A_{001}}{2}\right|^{2/3}.$$

On the right-hand side of this equation, A_{001} alone is a function of $\mathbf{d}$. Hence the maximum of $C(\mathbf{d})$ with respect to $\mathbf{d}$ is achieved by $\mathbf{d}$ that maximizes $|A_{001}|$ under the constraint (4). Using the expression (12) for A_{001}, we see that such $\mathbf{d}$ is parallel to $W^{-1}(\partial G/\partial \mathbf{v})$, i.e.

$$\mathbf{d} = -W^{-1}(\partial G/\partial \mathbf{v})/\alpha, \tag{17}$$

or its negative, where α is a positive scalar defined in such a manner that eqn (4) is satisfied. By substituting eqns (5) and (13) into eqn (17), we obtain the critical imperfection pattern $\mathbf{d}$ for our example problem:

$$\mathbf{d} = (-0.28404, -0.26061, -0.28404, 0.26061, 0.56812, 0, 0.43592EA, -0.43592EA)^{\mathrm{T}}. \tag{18}$$

Thus the critical imperfection pattern $\mathbf{d}$ has been computed by referring only to A_{001} in eqn (12). The other coefficients, such as A_{300} and A_{110}, which appeared in the derivation, need not be evaluated.

3. THEORY

A method for determining the worst initial imperfection against structures is introduced in this section. We consider geometrically non-linear equilibrium equations of a structure

under proportional loadings

$$f \cdot \mathbf{f}_0 = \mathbf{F}(\mathbf{u}, \mathbf{v}), \tag{19}$$

where $f \in \mathscr{R}^1$ indicates the loading parameter ($\mathscr{R}^1$ is the one-dimensional real space), $\mathbf{f}_0 \in \mathscr{R}^n$ is a constant loading pattern vector, $\mathbf{u} \in \mathscr{R}^n$ is the nodal displacement vector, $\mathbf{v} \in \mathscr{R}^p$ the imperfection parameter vector, $\mathbf{F} \in \mathscr{R}^n$ is sufficiently smooth (e.g. analytic) non-linear function in $\mathbf{u}$ and $\mathbf{v}$; n is the number of degrees of freedom and p the number of imperfection parameters. Note that the imperfection parameters are regarded as independent variables. Solutions of these equilibrium equations, which consist of $(f, \mathbf{u}) \in \mathscr{R}^1 \times \mathscr{R}^n$ satisfying eqn (19), make up equilibrium paths. These paths and critical points $(f_c, \mathbf{u}_c)$ are determined as functions in the imperfections $\mathbf{v}$.

Remark 3.1. We consider only proportional loading here, though more general loadings described by

$$\mathbf{F}_*(f, \mathbf{u}, \mathbf{v}) = \mathbf{0}$$

which involve the loading parameter f implicitly, can be implemented by replacing $\mathbf{f}_0$ with $\partial \mathbf{F}_*/\partial f$ in the present analysis. □

We consider a critical point $(f_c^0, \mathbf{u}_c^0)$ of the perfect system with $\mathbf{v} = \mathbf{v}^0$ that governs its load-bearing capacity, where $\mathbf{v}^0$ denotes the imperfection parameter vector for the perfect system; the Jacobian J of $\mathbf{F}$, known as the tangent-stiffness matrix, is singular at $(f_c^0, \mathbf{u}_c^0, \mathbf{v}^0)$:

$$\det \{J(f_c^0, \mathbf{u}_c^0, \mathbf{v}^0)\} = 0,$$

where

$$J = J(f, \mathbf{u}, \mathbf{v}) = [J_{ij}] = \left(\frac{\partial F_i}{\partial u_j}\right).$$

For an imperfect structure described by imperfection parameter $\mathbf{v}$, the critical point moves to $(f_c, \mathbf{u}_c)$, which is determined similarly by eqn (19) and

$$\det \{J(f_c, \mathbf{u}_c, \mathbf{v})\} = 0. \tag{20}$$

We write

$$f_c = f_c^0 + \hat{f}_c,$$

where $\hat{f}_c$ is the increment of the critical load f_c.

The imperfection is expressed in terms of the increment of $\mathbf{v}$ from the perfect state $\mathbf{v}^0$:

$$\varepsilon \mathbf{d} = \mathbf{v} - \mathbf{v}^0 \tag{21}$$

with an imperfection pattern vector $\mathbf{d}$ normalized as

$$\mathbf{d}^{\mathrm{T}} W \mathbf{d} = 1, \tag{22}$$

where W is a positive definite matrix to be specified in accordance with the design principle to be employed and ε is the magnitude of imperfection.

We formulate the problem of finding the critical imperfection as that of finding the imperfection pattern vector $\mathbf{d}$ that minimizes critical loads f_c (or $\hat{f}_c$) under the conditions of eqns (19), (20) and (22).

Remark 3.2. As is evident from our problem formulation above, we focus solely on the sensitivity of f_c on the imperfections. In practical applications, however, other aspects

of design demands, such as the allowable deformation limit, are equally important. The formulation and the implementation of these issues will require further studies. □

Usually critical points of structures are divided into either simple or multiple critical ones according to the rank deficiency of J. Hereafter we assume that $(f_c^0, \mathbf{u}_c^0)$ is a simple critical point of the perfect system; that is, the rank of J equals $n-1$ at $(f, \mathbf{u}, \mathbf{v}) = (f_c^0, \mathbf{u}_c^0, \mathbf{v}^0)$. Then there exists a unique vector $\boldsymbol{\xi}$ with the properties

$$\boldsymbol{\xi}^T J = \mathbf{0}^T, \quad \boldsymbol{\xi}^T \boldsymbol{\xi} = 1 \quad \text{and} \quad \boldsymbol{\xi}^T \mathbf{f}_0 \geq 0.$$

Also exists a vector $\boldsymbol{\eta}$, unique up to a scalar multiple, such that

$$J\boldsymbol{\eta} = \mathbf{0}. \tag{23}$$

Furthermore, we fix an arbitrary basis $\{\boldsymbol{\eta}_1, \boldsymbol{\eta}_2, \ldots, \boldsymbol{\eta}_n\}$ of $\mathscr{R}^n$ such that $\boldsymbol{\eta}_1 = \boldsymbol{\eta}$. Then $\mathbf{u}$ can be expressed uniquely as

$$\mathbf{u} = \mathbf{u}_c^0 + w\boldsymbol{\eta} + \sum_{j=2}^{n} w_j \boldsymbol{\eta}_j$$

and the nodal displacement is described by $\mathbf{w} = (w_1, w_2, \ldots, w_n)^T$, where $w = w_1$.

Remark 3.3. In the special case with J being symmetric, as in finite-element analysis, the distinguished vectors $\boldsymbol{\xi}$ and $\boldsymbol{\eta}$ as well as the basis of $\mathscr{R}^n$ above can be associated with the eigenvectors of J. Namely, the orthogonal eigenvector matrix

$$H = (\boldsymbol{\eta}_1, \boldsymbol{\eta}_2, \ldots, \boldsymbol{\eta}_n),$$

which is made up of eigenvectors $\boldsymbol{\eta}_i$ of J, diagonalizes J:

$$H^T J H = \operatorname{diag}[\lambda_1, \lambda_2, \ldots, \lambda_n],$$

where λ_i denotes the ith eigenvalue of J: $J\boldsymbol{\eta}_i = \lambda_i \boldsymbol{\eta}_i$ $(i = 1, 2, \ldots, n)$. It may be assumed that $\lambda_1 = 0$ and $\lambda_i \neq 0$ $(i = 2, 3, \ldots, n)$. Then $\boldsymbol{\xi} = \boldsymbol{\eta} = \boldsymbol{\eta}_1$ and $\{\boldsymbol{\eta}_1, \boldsymbol{\eta}_2, \ldots, \boldsymbol{\eta}_n\}$ is an orthogonal basis of $\mathscr{R}^n$. □

We now reduce the whole system of equations to a single equation in the variable w by means of the Lyapunov–Schmidt decomposition (e.g. Sattinger, 1979; Golubitsky and Schaeffer, 1985) of eqn (19) at $(f_c^0, \mathbf{u}_c^0)$. If we express the loading parameter f in terms of its increment $\hat{f}$ from f_c^0 as

$$f = f_c^0 + \hat{f},$$

$(\hat{f}, \mathbf{w}) = (0, \mathbf{0})$ corresponds to the critical point of the perfect structure. We employ the projection matrices $\boldsymbol{\xi}\boldsymbol{\xi}^T$ and $I_n - \boldsymbol{\xi}\boldsymbol{\xi}^T$, where I_n denotes the unit matrix of order n. On premultiplying eqn (19) with these matrices and using the new variables $\hat{f}$ and $\mathbf{w}$, we arrive at the equations for the null space

$$\boldsymbol{\xi}\left\{(\boldsymbol{\xi}^T \mathbf{f}_0)(f_c^0 + \hat{f}) - \boldsymbol{\xi}^T \mathbf{F}\left(\mathbf{u}_c^0 + w\boldsymbol{\eta} + \sum_{j=2}^{n} w_j \boldsymbol{\eta}_j, \mathbf{v}\right)\right\} = \mathbf{0}, \tag{24}$$

and those for the rank space

$$(I_n - \boldsymbol{\xi}\boldsymbol{\xi}^T)\mathbf{f}_0(f_c^0 + \hat{f}) - (I_n - \boldsymbol{\xi}\boldsymbol{\xi}^T)\mathbf{F}\left(\mathbf{u}_c^0 + w\boldsymbol{\eta} + \sum_{j=2}^{n} w_j \boldsymbol{\eta}_j, \mathbf{v}\right) = \mathbf{0}. \tag{25}$$

The derivatives of eqn (25) with respect to w_j are computed as

$$(I_n - \boldsymbol{\xi}\boldsymbol{\xi}^T) J\boldsymbol{\eta}_j = J\boldsymbol{\eta}_j, \quad j = 2, 3, \ldots, n.$$

Because $\eta_1, \eta_2, \ldots, \eta_n$ are linearly independent and eqn (23) holds, these derivatives are also linearly independent and hence eqn (25) can be solved with the use of the implicit function theorem as

$$w_j = w_j(\hat{f}, w, \mathbf{v}), \quad j = 2, 3, \ldots, n.$$

On substituting this into eqn (24) and noting that $\xi \neq \mathbf{0}$, we obtain a single equation

$$G(\hat{f}, w, \mathbf{v}) = (\xi^{\mathrm{T}}\mathbf{f}_0)(f_c^0 + \hat{f}) - \xi^{\mathrm{T}}\mathbf{F}\left(\mathbf{u}_c^0 + w\eta + \sum_{j=2}^{n} w_j(\hat{f}, w, \mathbf{v})\eta_j, \mathbf{v}\right) = 0, \tag{26}$$

which is known as the bifurcation equation if $\mathbf{v} = \mathbf{v}^0$.

We hereby regard the imperfection magnitude ε as an independent variable in eqn (26) and put

$$\bar{G}(\hat{f}, w, \varepsilon) = G(\hat{f}, w, \mathbf{v}^0 + \varepsilon\mathbf{d}).$$

As assumed earlier, F_i $(i = 1, 2, \ldots, n)$ are sufficiently smooth and so is the function $\bar{G}(\hat{f}, w, \varepsilon)$. We may then grasp the essential nature of eqn (26) by expanding $\bar{G}$ into a power series involving appropriate number of terms (see Iooss and Joseph, 1981):

$$\bar{G}(\hat{f}, w, \varepsilon) = \sum_{i=0}\sum_{j=0}\sum_{k=0} A_{ijk} w^i \hat{f}^j \varepsilon^k, \tag{27}$$

where

$$A_{ijk} = A_{ijk}(\mathbf{d}) = \frac{1}{i!j!k!} \cdot \frac{\partial \bar{G}^{i+j+k}}{\partial w^i \, \partial \hat{f}^j \, \partial \varepsilon^k}\bigg|_{(\hat{f}, w, \varepsilon) = (0,0,0)}$$

The coefficients A_{ijk} $(k \geqslant 1)$ are functions of $\mathbf{d}$ but such is not the case for A_{ij0}. Since $(\hat{f}, w, \varepsilon) = (0, 0, 0)$ corresponds to the critical point from the perfect system, we have

$$A_{000} = 0, \quad A_{100} = 0, \quad A_{010} = \xi^{\mathrm{T}}\mathbf{f}_0. \tag{28}$$

The lowest order term in ε, which governs the imperfection sensitivity as we will see later, is computed from eqn (26) as

$$A_{001} = \frac{\partial \bar{G}}{\partial \varepsilon} = -\xi^{\mathrm{T}} B \mathbf{d}, \tag{29}$$

where

$$B = [B_{ij}] = \left(\frac{\partial F_i}{\partial v_j}\right), \quad i = 1, 2, \ldots, n, \; j = 1, 2, \ldots, p,$$

will be called the imperfection sensitivity matrix; B is real but neither square nor symmetric. We assume $A_{001} \neq 0$ in the following, since $A_{001} = 0$ means that the effect of imperfections is of the second or higher order.

Note that the condition (20) for a critical point for the whole equilibrium equations reduces to $\partial \bar{G}/\partial w = 0$ for the bifurcation equation. At a critical point of an imperfect structure, $(\hat{f}, w)$ satisfies

$$\bar{G} = 0, \quad \frac{\partial \bar{G}}{\partial w} = 0. \tag{30}$$

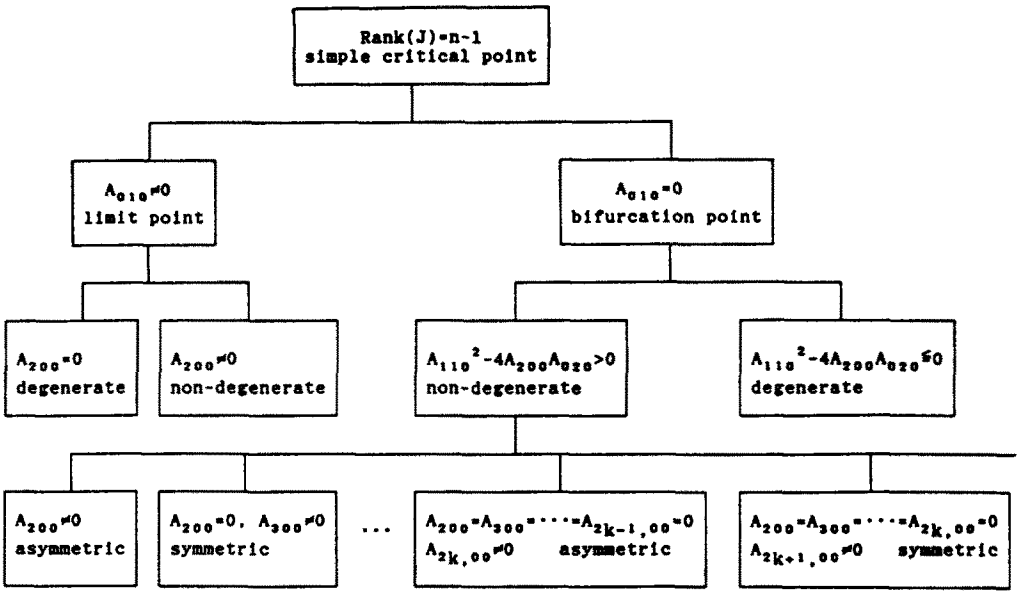

Fig. 3. Classification of simple critical points.

As shown in Fig. 3, simple critical points are classified into the following major types: limit points, asymmetric bifurcation points, stable- and unstable-symmetric bifurcation points. A critical point is said to be of mth order if

$$A_{000} = A_{100} = \cdots = A_{m-1,00} = 0, \quad A_{m00} \neq 0.$$

Critical points are assumed to be non-degenerate in this section, that is, $A_{200} \neq 0$ for a limit point, and $A_{110}^2 - 4A_{200}A_{020} > 0$ for a bifurcation point.

The solution of eqn (30) is given asymptotically for ε small as follows according to the above classification (see the Appendix for the derivation).

(i) For a limit point,

$$\hat{f}_c \approx \frac{-A_{001}}{A_{010}}\varepsilon. \tag{31}$$

(ii) For an asymmetric bifurcation point of order two,

$$\hat{f}_c \approx \pm\{4|A_{200}|A_{001}/(A_{110}^2 - 4A_{200}A_{020})\}^{1/2}\{\text{sign}\,(A_{200})\varepsilon\}^{1/2}, \tag{32}$$

where sign $(\cdot)$ denotes the sign of the variable in the parentheses. Critical loads exist for the imperfect system only if the sign of imperfection magnitude ε coincides with that of A_{200}.

(iii) For a symmetric bifurcation point of odd order m (≥ 3),

$$\hat{f}_c \approx \frac{-m}{A_{110}} A_{m00}^{1/m} \left|\frac{A_{001}}{m-1}\right|^{1-1/m} \varepsilon^{1-1/m}. \tag{33}$$

(iv) For an asymmetric bifurcation point of even order m (≥ 4),

$$\hat{f}_c \approx \frac{\pm m}{A_{110}} |A_{m00}|^{1/m} \left|\frac{A_{001}}{m-1}\right|^{1-1/m} \{\text{sign}\,(A_{m00})\varepsilon\}^{1-1/m}. \tag{34}$$

Simple bifurcation points of order greater than three are rare in structures, though we included this case here for theoretical completeness.

On the right-hand sides of eqns (31), (32), (33) and (34), A_{001} alone is a function of $\mathbf{d}$. Hence the maximum of $|\hat{f}_c|$ with respect to $\mathbf{d}$ is achieved by $\mathbf{d}$ that maximizes $|A_{001}|$. In view of eqn (29) we see that $|A_{001}|$, and hence $|\hat{f}_c|$, is maximized under constraint (22) when $\mathbf{d}$ is chosen to be parallel to $W^{-1}B^{\mathrm{T}}\xi$; that is,

$$\mathbf{d} = -W^{-1}B^{\mathrm{T}}\xi/\alpha, \tag{35}$$

where

$$\alpha = \{\xi^{\mathrm{T}}BW^{-1}B^{\mathrm{T}}\xi\}^{1/2} > 0. \tag{36}$$

For this critical imperfection pattern, A_{001} equals

$$A_{001} = \alpha > 0 \tag{37}$$

by eqn (29). It is to be noted that the critical imperfection pattern is given by eqn (35) irrespective of the type of simple critical points.

For a limit point, substituting eqn (37) into eqn (31) and using eqn (28), we obtain the first-order approximation of $\hat{f}_c$ as

$$\hat{f}_c \approx -\alpha\varepsilon/(\xi^{\mathrm{T}}\mathbf{f}_0), \tag{38}$$

where $A_{010} = \xi^{\mathrm{T}}\mathbf{f}_0 > 0$. This shows that the critical load increment is linearly proportional to ε. The capacity f_c deteriorates for positive ε but increases for negative ε, as shown in Fig. 4(a).

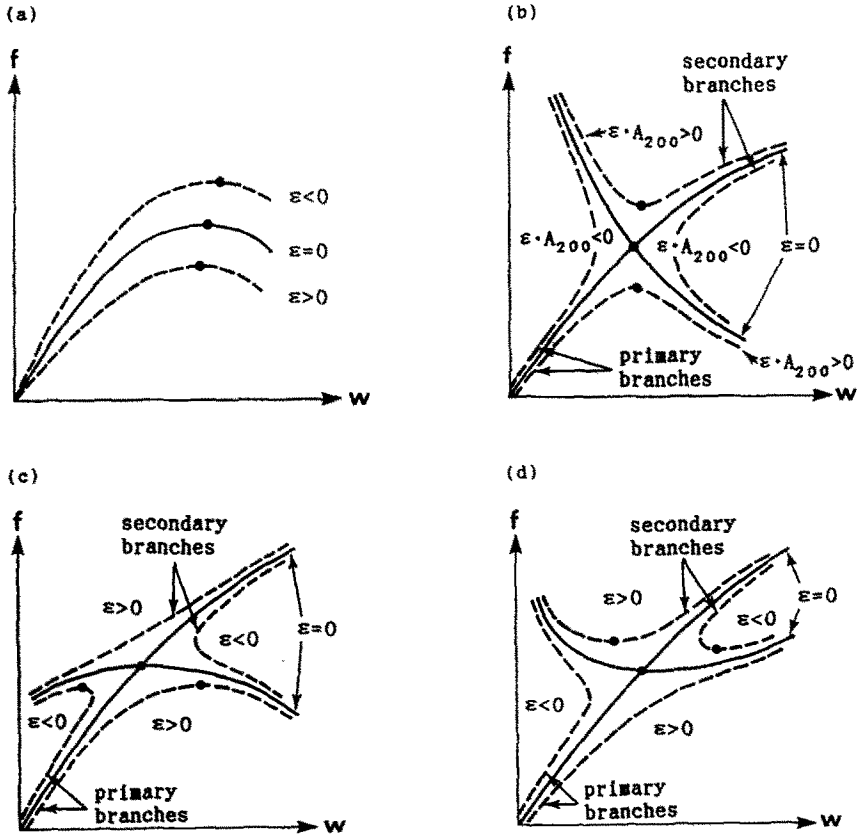

Fig. 4. Effects of ε on simple critical points. (a) Limit point, (b) asymmetric bifurcation point, (c) unstable-symmetric bifurcation point, (d) stable-symmetric bifurcation point.

For a bifurcation point, the branches for an imperfect system consist of a pair of a primary (natural) branch and a secondary (complementary) branch (see Fig. 4). Only the primary branch which is encountered in a natural loading sequence starting from $f = 0$ is of physical and practical importance.

For an asymmetric bifurcation point, the primary branch of an imperfect system either has a limit (maximum) point or has no critical point according to whether $\varepsilon \cdot A_{200}$ is positive or negative. Only the former case is of physical and engineering importance, but the sign of ε related to this case cannot be known *a priori* unless A_{200} is computed at a tedious cost. In actual analysis, we may trace the primary paths with ε both positive and negative instead of computing A_{200}.

For an unstable-symmetric bifurcation point, at which $A_{m00}A_{110} > 0$, a primary branch has a limit (maximum) point of f that governs the load-bearing capacity. The capacity f_c is reduced for both positive and negative ε. [Note: for $m = 3$, this criterion for stability based on the sign of $A_{300}A_{110}$ agrees with that given by Thompson and Hunt (1973) though this may not be apparent.]

For a stable-symmetric bifurcation point, at which $A_{m00}A_{110} < 0$, a limit (minimum) point of f exists on the secondary branch of an imperfect system. The primary branch of an imperfect system, which is constantly rising, is stable in the neighborhood of the bifurcation point of the perfect system. Thus the critical imperfection pattern computed by our method does not seem to have direct practical importance in this case. See also Remark 3.5 below.

In practice, the imperfection parameters are often divided into different categories so as to implement various kinds of imperfections with diversified physical properties. Then we partition the parameters into N categories,

$$\mathbf{v} = (\mathbf{v}_1^{\mathrm{T}}, \mathbf{v}_2^{\mathrm{T}}, \ldots, \mathbf{v}_N^{\mathrm{T}})^{\mathrm{T}}$$

and accordingly put

$$\mathbf{v}^0 = (\mathbf{v}_1^{0\mathrm{T}}, \mathbf{v}_2^{0\mathrm{T}}, \ldots, \mathbf{v}_N^{0\mathrm{T}})^{\mathrm{T}}, \quad \mathbf{d} = (\mathbf{d}_1^{\mathrm{T}}, \mathbf{d}_2^{\mathrm{T}}, \ldots, \mathbf{d}_N^{\mathrm{T}})^{\mathrm{T}}, \quad B = [B_1, B_2, \ldots, B_N].$$

Note that $\mathbf{d}$ and B are decomposed compatibly with the definition of $\mathbf{v}$. The imperfection patterns $\mathbf{d}_k$ $(k = 1, 2, \ldots, N)$ are defined as

$$\varepsilon \mathbf{d}_k = \mathbf{v}_k - \mathbf{v}_k^0, \quad k = 1, 2, \ldots, N,$$

and normalized as

$$\mathbf{d}_k^{\mathrm{T}} W_k \mathbf{d}_k = 1, \quad k = 1, 2, \ldots, N.$$

All results obtained above for one category of imperfections apply to each category, and the critical imperfection pattern for each category is given by

$$\mathbf{d}_k = -W_k^{-1} B_k^{\mathrm{T}} \boldsymbol{\xi} / \alpha_k, \quad k = 1, 2, \ldots, N, \tag{39}$$

where

$$\alpha_k = \{\boldsymbol{\xi}^{\mathrm{T}} B_k W_k^{-1} B_k^{\mathrm{T}} \boldsymbol{\xi}\}^{1/2} > 0, \quad k = 1, 2, \ldots, N.$$

The variable α_k represents the influence of the imperfection in the kth category to the critical load increment $\hat{f}_c$; the kth category has significant or insignificant influence on $\hat{f}_c$ according to whether α_k is large or small in value.

For a limit point, $\hat{f}_c$ is calculated from eqn (38) as a superposition of the effects from the categories:

$$\hat{f}_c \approx -\left(\sum_{k=1}^{N} \alpha_k\right) \varepsilon \Big/ (\boldsymbol{\xi}^{\mathrm{T}} \mathbf{f}_0). \tag{40}$$

Remark 3.4. In our problem formulation we have assumed that the weight matrices W_k $(k = 1, \ldots, N)$ are given *a priori*. From the mathematical point of view, these matrices may be arbitrarily chosen as long as they are positive definite. The choice of the weight matrices should reflect the design principle and the technological constraints. For example, W_k may be chosen "small" if the imperfection $\mathbf{v}_k$ in the kth category is expected to be small for some technological reasons. Not surprisingly the resulting critical imperfection vectors $\mathbf{d}_k$ are substantially affected by the choice of W_k; note, however, that B_k and ξ in eqn (39) are independent of W_k. □

Remark 3.5. It would be in order here to mention the theory of universal unfolding due to Golubitsky and Schaeffer (1985). The theory identifies those imperfections which lead to qualitatively different bifurcation phenomena.

Recall that we have obtained a single equation (26) which describes the local behavior around the critical point $(f_c^0, \mathbf{u}_c^0, \mathbf{v}^0)$, and suppose, for concreteness, that this point is a stable-symmetric bifurcation point. According to the theory, all the qualitatively different imperfect bifurcation diagrams are described by a two-parameter family of imperfections, called a universal unfolding. For example, the family of

$$U(\hat{f}, w, \beta_1, \beta_2) = w^3 - \hat{f}w + \beta_1 + \beta_2 w^2$$

parameterized by (β_1, β_2) is qualified as such. Note $(\beta_1, \beta_2) = (0, 0)$ corresponds to the perfect system. The theory says that $\bar{G}$ in eqn (27) is obtained from U in the sense that $\bar{G}$ factors through U [see Golubitsky and Schaeffer (1985) for the precise meaning]. However, this result does not seem to have a direct application in the present analysis of critical imperfections.

Instead we will make use of this result to explain a subtle point of our formulation of the critical imperfection. It is known that the primary branch of $U(\hat{f}, w, \beta_1, \beta_2) = 0$ has a kink (i.e. a pair of maximal and minimal limit points) if (β_1, β_2) belongs to the region

$$K = \{(\beta_1, \beta_2) | 0 < \beta_1 < \beta_2^3/27 \quad \text{or} \quad \beta_2^3/27 < \beta_1 < 0\}.$$

In our problem formulation we have fixed the direction $\mathbf{d}$ of imperfection $\mathbf{v} = \mathbf{v}_0 + \varepsilon\mathbf{d}$ as in eqn (21) and considered the asymptotic behavior as $|\varepsilon|$ tends to 0. For the problem described by U, we put $(\beta_1, \beta_2) = \varepsilon(d_1, d_2)$ and let $|\varepsilon|$ tend to 0. It is easy to see that for any fixed (d_1, d_2), (β_1, β_2) lies outside of the region K if $|\varepsilon|$ is sufficiently small. This explains why the primary branch with a kink has been ignored in our analysis. □

Remark 3.6. In correspondence to the change $\hat{f}_c$ in load-bearing capacity given in eqns (31) to (34), the magnitude of the change in displacement $\mathbf{u}_c - \mathbf{u}_c^0$ is computed from eqn (30) as being the order of ε if $m = 1$, and of $\varepsilon^{1/m}$ if $m \geqslant 2$; when $m \geqslant 3$, this is larger in order than $\hat{f}_c$. □

4. NUMERICAL EXAMPLES

Case studies on simple structures with various types of simple critical points are performed by means of the proposed method for determining the worst imperfection. Remember that the critical imperfection pattern $\mathbf{d}$ is given by eqn (35) regardless of types of points, whereas imperfection sensitivity varies with types. In these examples, we shall deal with proportional loading problems with symmetric Jacobian matrices, which are fairly tractable and conventional as explained in Remarks 3.1 and 3.3.

Limit point and unstable-symmetric bifurcation point

Figure 1 shows the shallow arch (a) whose load-bearing capacity is governed by a limit point and the non-shallow one (b) by an unstable-symmetric bifurcation point. The locations of the nodes and the sectional and material properties shown in (a) and (b) denote their perfect cases.

Equilibrium equations under a vertical load f are given by eqn (1) in Section 2.

Imperfection parameter vector is chosen to be

$$\mathbf{v} = (\mathbf{v}_1^T, \mathbf{v}_2^T, \mathbf{v}_3^T, \mathbf{v}_4^T, \mathbf{v}_5^T)^T,$$

where

$$\mathbf{v}_k = (x_k, y_k)^T, \quad k = 1, 2, 3; \quad \mathbf{v}_4 = (EA_1); \quad \mathbf{v}_5 = (EA_2).$$

In the perfect cases

$$\mathbf{v}^0 = \begin{cases} (-1, 1, 1, 1, 0, 0, EA, EA)^T & \text{for the shallow arch} \\ (-1, 3, 1, 3, 0, 0, EA, EA)^T & \text{for the non-shallow arch.} \end{cases}$$

We set

$$W_1 = W_2 = W_3 = I_2; \quad W_4 = W_5 = 1/(EA)^2. \tag{41}$$

The tangent-stiffness matrix is given by eqn (6). Eigenvalues of J are computed as

$$\lambda_i = \tfrac{1}{2}[J_{xx} + J_{yy} + (-1)^i \{(J_{xx} - J_{yy})^2 + 4J_{xy}^2\}^{1/2}], \quad i = 1, 2; \quad \lambda_1 < \lambda_2.$$

The smaller eigenvalue λ_1 is relevant to the critical point determining the load-bearing capacity, and its associated eigenvector is

$$\xi = \eta = [J_{xy}/\{J_{xy}^2 + (\lambda_1 - J_{xx})^2\}^{1/2}, (\lambda_1 - J_{xx})/\{J_{xy}^2 + (\lambda_1 - J_{xx})^2\}^{1/2}]^T.$$

Equation (1) of the perfect shallow arch yields its equilibrium path (f versus y curve) shown in Fig. 5 by a solid line. The load-bearing capacity of this path is governed by a limit point B, where $\xi = \eta = (0, 1)^T$ and $(f_c^0, x_c^0, y_c^0) = (0.18740EA, 0, 0.49018)$.

We computed the critical imperfection pattern vector $\mathbf{d}$ from eqn (39) with the use of eqn (41):

$$\mathbf{d} = (-1/\sqrt{2}, -1/\sqrt{2}, 1/\sqrt{2}, -1/\sqrt{2}, 0, 1, -EA, -EA)^T. \tag{42}$$

This imperfection makes the arch less flat for $\varepsilon < 0$, thereby enhancing its vertical stiffness against snap-through-type collapse, and for $\varepsilon > 0$, it makes the arch even flatter and reduces the stiffness. The imperfection pattern theoretically obtained here, therefore, is sound through physical viewpoints as well. Broken lines in Fig. 5 show the equilibrium paths

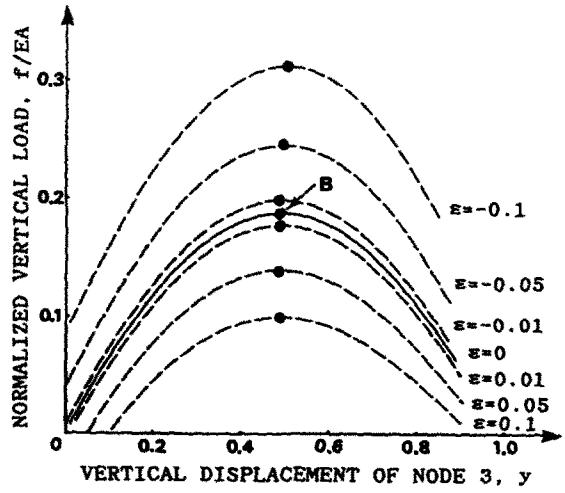

Fig. 5. f versus y curves for the shallow arch with and without imperfections (limit point).

computed for the pattern **d** in eqn (42) with imperfection magnitudes of $\varepsilon = \pm 0.01$, ± 0.05 and ± 0.1.

The increment $\hat{f}_c$ of f_c associated with **d** of eqn (42) is computed from eqn (40) with (41) as

$$\hat{f}_c \approx -\left(\sum_{k=1}^{5} \alpha_k\right)\varepsilon \Big/ (\boldsymbol{\xi}^{\mathrm{T}}\mathbf{f}_0) = -1.0577EA\varepsilon, \tag{43}$$

where the α_k ($k = 1, 2, \ldots, 5$), denoting the influence of the imperfection in the kth category on $\hat{f}_c$, are

$$(\alpha_1, \alpha_2, \alpha_3, \alpha_4, \alpha_5) = EA(0.25491, 0.25491, 0.36050, 0.09370, 0.09370).$$

Since α_3 is the greatest among α_k, the imperfection of (x_3, y_3) reduces $\hat{f}_c$ most rapidly. The imperfections of EA_1 and EA_2 with the smallest α_k, in contrast, are least influential.

Figure 6 shows the interrelationship between the normalized load-bearing capacity f_c/f_c^0 and the magnitude of imperfection ε. The solid line denotes the critical loads estimated theoretically from eqn (43), while the closed circles (●) denote those computed from eqn (1) for the imperfections. The estimation correlates well with the critical loads of imperfect arches, although the discrepancy enlarges as ε increases due to the approximation errors in the incremental eqn (43), which includes only the first-order term.

For the non-shallow arch, we obtained equilibrium paths (f versus x curves) in Fig. 2. As we have described in Section 2, the paths consist of a main (trivial) path and a pair of bifurcation paths branching at the simple unstable-symmetric bifurcation point A. The critical eigenvector at A is $\boldsymbol{\xi} = \boldsymbol{\eta} = (1, 0)^{\mathrm{T}}$ and $(f_c^0, x_c^0, y_c^0) = (0.24776EA, 0, 0.44735)$. The critical imperfection pattern is computed from eqn (39) as

$$\mathbf{d} = (-0.73685, -0.67606, -0.73685, 0.67606, 1, 0, EA, -EA)^{\mathrm{T}}, \tag{44}$$

which imbalances horizontal stiffness and hence triggers buckling. The dashed lines in Fig. 2 denote the paths computed for **d** of eqn (44) for $\varepsilon = \pm 0.01$, ± 0.05 and ± 0.1. Note that **d** of eqn (44) computed for the five categories of weight matrices of eqn (41) is different from **d** of eqn (18) computed for the one category of weight matrix of eqn (5). The weight matrices and categories, which affect greatly the resulting critical imperfection pattern, must be chosen on the basis of sound engineering judgements.

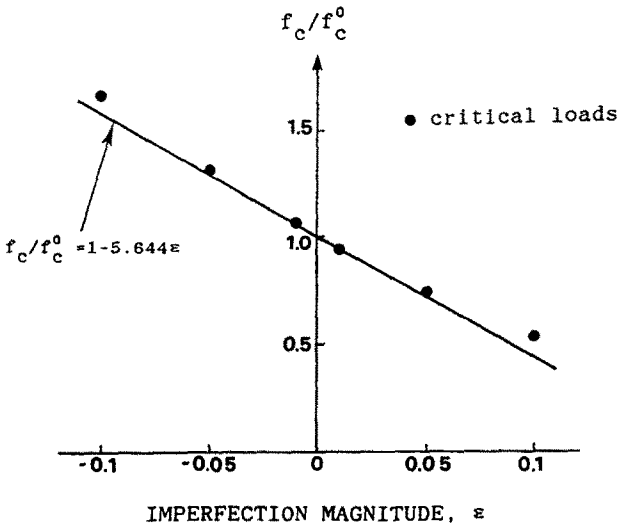

Fig. 6. f_c/f_c^0 versus ε relationship for the shallow arch (limit point).

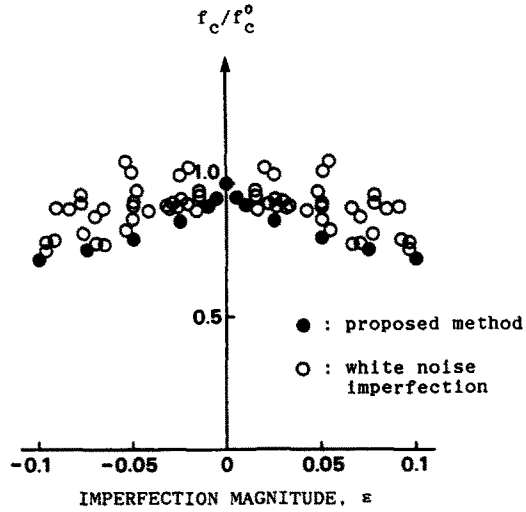

Fig. 7. f_c/f_c^0 versus ε relationship for the non-shallow arch (unstable-symmetric bifurcation point).

The increment $\hat{f}_c$ of f_c related to $\mathbf{d}$ of (44) is computed from eqn (33):

$$\hat{f}_c \approx -C\left(\sum_{k=1}^{5} \alpha_k\right)^{2/3} \varepsilon^{2/3} \tag{45}$$

with a positive constant C independent of ε and

$$(\alpha_1, \alpha_2, \alpha_3, \alpha_4, \alpha_5) = EA(0.04292, 0.04292, 0.06325, 0.04853, 0.04853).$$

Since α_3 is the greatest among α_k, the imperfection of (x_3, y_3) has the greatest influence on $\hat{f}_c$.

Figure 7 shows the f_c/f_c^0 versus ε relationship. The open circles (○) indicate f_c computed from eqns (1) for imperfections chosen based on white noise, and the closed circles (●) for the critical imperfection in eqn (44) by the proposed method. The latter f_c values are smaller than the former for the same imperfection magnitude ε; this assesses the validity of this method. The critical load f_c computed by the method decreases as theoretically predicted in eqn (45), in accordance with the two-thirds power law of Koiter (1945).

The influence of the x_3 and y_3 values on the load-bearing capacity of the non-shallow arch was investigated by changing their values in the ranges $-0.5 \leqslant x_3 \leqslant 0.5$ and $-0.5 \leqslant y_3 \leqslant 0.5$ at a fine mesh with other imperfections kept fixed. Figure 8 shows the

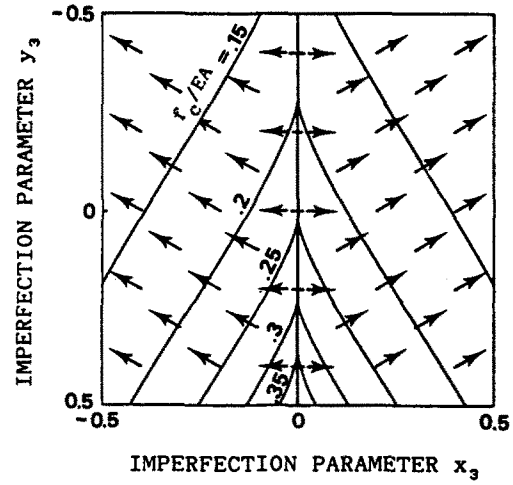

Fig. 8. Contours of f_c as a function of x_3 and y_3 for the non-shallow arch.

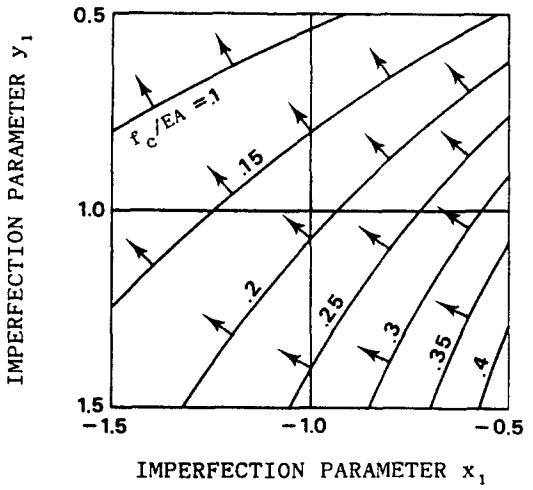

Fig. 9. Contours of f_c as a function of x_1 and y_1 for the shallow arch.

contour lines of f_c values and the directions of the worst imperfection computed by eqn (35). The numerals at the lines denote the f_c values and the arrows indicate the worst direction of (dx_3, dy_3) at each point (x_3, y_3). The center $(x_3, y_3) = (0, 0)$ of this figure corresponds to the perfect non-shallow arch; the solid (respectively broken) arrows indicate that the load-bearing capacity is governed by a limit (respectively bifurcation) point.

Figure 9 shows the case of the shallow arch for various values of (x_1, y_1). The center $(x_1, y_1) = (-1, 1)$ of this figure is associated with the perfect shallow arch. In Figs 8 and 9, the theoretically computed imperfection vectors are orthogonal to the contour lines, i.e. directed toward the steepest decline of f_c; this verifies the validity of our method.

Asymmetric bifurcation point

Consider the propped cantilever of Fig. 10 comprising a truss member, simply supported at a rigid foundation and supported by horizontal and vertical springs. The equilibrium equations under a vertical load f are

$$f\begin{pmatrix}0\\1\end{pmatrix} = \begin{pmatrix}EA(1/L-1/\hat{L})(x-x_1)+F_{sx}\\EA(1/L-1/\hat{L})(y-y_1)+F_{sy}\end{pmatrix}, \tag{46}$$

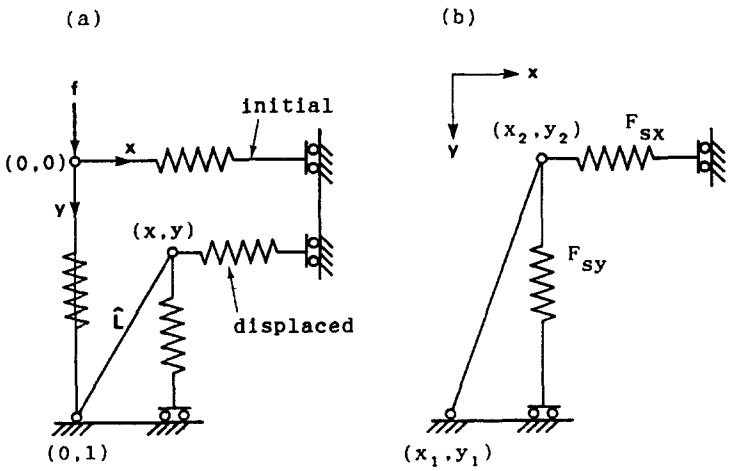

Fig. 10. Propped cantilever. (a) perfect system, (b) imperfect system.

where

$$L = \{(x_2-x_1)^2+(y_2-y_1)^2\}^{1/2}; \quad \hat{L} = \{(x-x_1)^2+(y-y_1)^2\}^{1/2};$$
$$F_{sx} = EA\{\beta_1+\beta_2(x-x_2)/L+\beta_3(x-x_2)^2/L^2\}; \quad F_{sy} = EA\beta_4(y-y_2)/L,$$

and (x, y) is the location of node 2 after displacement; and F_{sx} and F_{sy} are the horizontal and the vertical force exerted by the springs, respectively.

The imperfection parameter vector is

$$\mathbf{v} = (\mathbf{v}_1^T, \mathbf{v}_2^T, \mathbf{v}_3^T)^T,$$

where

$$\mathbf{v}_k = (x_k, y_k)^T, \quad k = 1,2; \quad \mathbf{v}_3 = (\beta_1, \beta_2, \beta_3, \beta_4)^T.$$

In the perfect case, we have

$$\mathbf{v}^0 = (0,1, \quad 0,0, \quad 0,1,1,1,)^T. \tag{47}$$

We set $W_1 = W_2 = I_2$; $W_3 = I_4$.

The equilibrium eqns (46) give the solution paths for the perfect cantilever as

$$\begin{cases} x = 0, \quad f/EA = 2y, \quad y < 1: \\ \quad \text{main path,} \\ y = 1-\{1/(x+2)^2-x^2\}^{1/2}, \quad f/EA = 1+x\{1/(x+2)^2-x^2\}^{1/2}, \quad x > -2: \\ \quad \text{bifurcation paths,} \end{cases} \tag{48}$$

and those for the imperfect cantilever as

$$y = y_1-|x-x_1|\cdot R(x),$$
$$f/EA = \beta_4(y_1-y_2)/L+\{F_{sx}(x)\ \text{sign}\ (x-x_1)/EA-\beta_4|x-x_1|/L\}R(x),$$
$$F_{sx}(x)/\{EA(x-x_1)\}+1/L > 0, \tag{49}$$

where

$$R(x) = [\{(x-x_1)/L+F_{sx}(x)/EA\}^{-2}-1]^{1/2}.$$

Figure 11 shows f versus x curves computed for the perfect cantilever. The curves consist of a main path and a pair of bifurcation paths branching at a simple asymmetric bifurcation point C. The critical eigenvector at C is $\boldsymbol{\xi} = \boldsymbol{\eta} = (1,0)^T$ and $(f_c^0, x_c^0, y_c^0) = (EA, 0, 1/2)$. The critical imperfection pattern $\mathbf{d}$ computed by eqn (39) is

$$\mathbf{d} = (-1,0, \quad 1,0, \quad -1,0,0,0)^T. \tag{50}$$

From eqn (32) the increment $\hat{f}_c$ of f_c related to $\mathbf{d}$ is

$$\hat{f}_c \approx C\left(\sum_{k=1}^{3}\alpha_k\right)^{1/2}(-\varepsilon)^{1/2}, \tag{51}$$

where C is a positive constant and $\alpha_k = EA$ $(k = 1,2,3)$. The three categories of imperfections, having the same α_k values, make the same asymptotic contributions to the critical load increment $\hat{f}_c$.

The dashed lines in Fig. 11 denote the paths computed from eqns (49) for $\mathbf{d}$ in eqn (50)

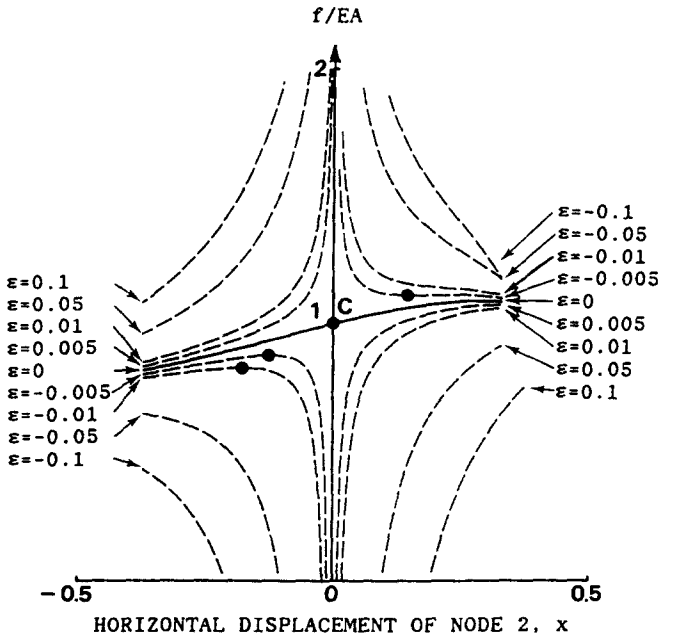

Fig. 11. f versus x curves for the propped cantilever with $\mathbf{v}^0$ in eqn (47) (asymmetric bifurcation point).

for $\varepsilon = \pm 0.005$, ± 0.01, ± 0.05 and ± 0.1. Each of the two paths with $\varepsilon = -0.005$ has a limit point in the vicinity of point C. This agrees with (51) which implies the existence of two neighboring limit points with opposite signs of $\hat{f}_c$. However, only one neighboring limit point was observed for $\varepsilon = -0.01$ and no such points were observed for the paths with $\varepsilon = -0.05$ and -0.1. This absence of limit points is due to the global non-linearity of the bifurcation behavior of the propped cantilever. Note that the proposed method focuses on the local asymptotic aspects of the bifurcation behavior and is expected to hold for sufficiently small ε, such as $\varepsilon = -0.005$ in this case.

Stable-symmetric bifurcation point

The propped cantilever with different spring properties is investigated. We choose

$$\mathbf{v}^0 = (0, 1, \quad 0, 0, \quad 0, 1, 0, 2)^T \tag{52}$$

as the perfect structure. The equilibrium eqns (46) yield the solution paths:

$$\begin{cases} x = 0, \quad f/EA = 3y, \quad y < 1: & \text{main path} \\ y = 1-(\frac{1}{4}-x^2)^{1/2}, \quad f/EA = 2-(\frac{1}{4}-x^2)^{1/2}: & \text{bifurcation paths} \end{cases} \tag{53}$$

for $\mathbf{v} = \mathbf{v}^0$, and the paths of eqns (49) for the imperfect structures.

Figure 12 shows f versus x curves for the perfect cantilever with $\mathbf{v}^0$ in eqn (52). The curves consist of a main (trivial) path and a pair of bifurcation paths, which branch from the main path at a simple stable-symmetric bifurcation point D. The critical eigenvector at D is $\boldsymbol{\xi} = \boldsymbol{\eta} = (1, 0)^T$ and $(f_c^0, x_c^0, y_c^0) = (3EA/2, 0, 1/2)$. The critical imperfection pattern $\mathbf{d}$ computed by eqn (39) is

$$\mathbf{d} = (-1, 0, \quad 1, 0, \quad -1, 0, 0, 0)^T. \tag{54}$$

The dashed lines in Fig. 12 denote the paths computed from eqn (49) with $\mathbf{v}^0$ in eqn (52), with the imperfection pattern in eqn (54), and with $\varepsilon = \pm 0.01$, ± 0.05 and ± 0.1.

From eqn (33) the increment $\hat{f}_c$ of the load-bearing capacity f_c related to $\mathbf{d}$ of eqn (54)

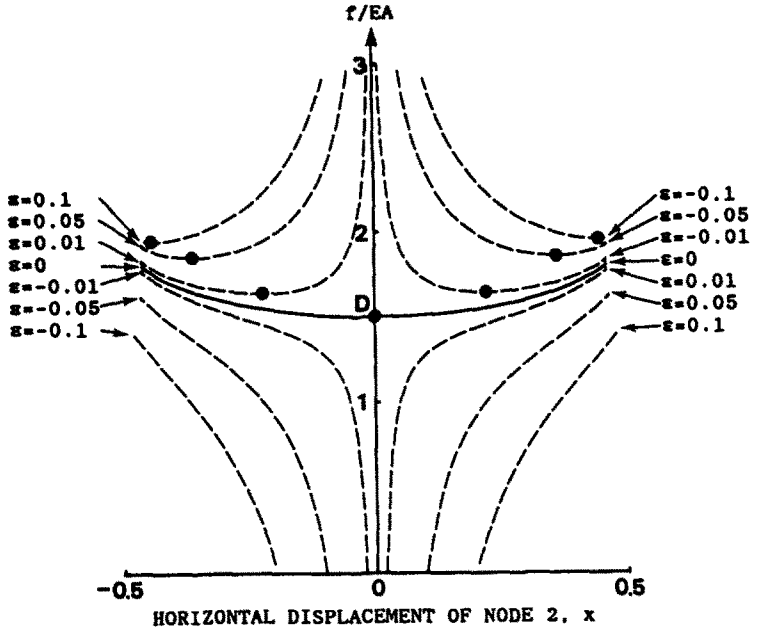

Fig. 12. f versus x curves for the propped cantilever with v^0 in eqn (52) (stable-symmetric bifurcation point).

is

$$\hat{f}_c \approx C\left(\sum_{k=1}^{3} \alpha_k\right)^{2/3} \varepsilon^{2/3}$$

with a positive constant C and $\alpha_k = EA\,(k = 1, 2, 3)$. Again, the three categories of imperfections have the same asymptotic influence on $\hat{f}_c$.

5. CONCLUDING REMARKS

A method is proposed for determining the critical (or worst) initial imperfection of structures. The first half of this paper is devoted to the theory of the method and the second half to its illustration with the use of simple example structures.

The critical imperfection pattern vector at a simple critical point is independent of the type of the point, being given by

$$\mathbf{d} = -W^{-1}B^{\mathrm{T}}\xi/\alpha,$$

where ξ is the critical eigenmode, B is the imperfection sensitivity matrix, and W is a weighting matrix.

The initial imperfections are divided into categories so as to implement various kinds of imperfections with diversified physical properties. The contribution of each category to the critical load increment $\hat{f}_c$ is characterized quantitatively by the variable α_k:

$$\alpha_k = \{\xi^{\mathrm{T}} B_k W_k^{-1} B_k^{\mathrm{T}} \xi\}^{1/2} > 0, \quad k = 1, 2, \ldots, N.$$

With the use of α_k, one can identify the imperfection parameters that greatly affect the critical loads. All kinds of imperfections can readily be implemented in the formulation, unlike most of the other techniques hitherto proposed for determining critical imperfections.

The types of critical points substantially influence the sensitivity of the critical load increment $\hat{f}_c$ to the imperfection magnitude ε. This conforms with the study of Thompson and Hunt (1973), which considered the sensitivity of a system with a potential energy

function to a few imperfection parameters. Our method is more versatile than their perturbation method in that it is applicable to a system which may or may not have a potential function and may involve a large number of imperfection parameters.

The method was applied to simple truss structures to assess its validity and usability. Simple calculations enabled us to arrive at the most favorable or unfavorable imperfections. The most influential imperfection parameter on critical loads was identified. The imperfections selected in this manner were physically feasible and, at the same time, altered the critical loads as predicted by the theory.

In this paper, we disregarded double (multiple) critical points in favor of simple ones. For double bifurcation points which arise due to geometric symmetry of systems, the determination of the critical imperfection pattern vector will require the concept of group symmetry (see Sattinger, 1979, 1980) and will be a topic of future research; see Murota and Ikeda (1990).

For customary cases where the tangent-stiffness matrix is symmetric, the critical imperfection patterns are expected to be calculated compatibly with finite-element analyses based on matrix-type formulation. The computational details will be reported in a forthcoming paper by Ikeda and Murota (1990) with applications to a practical large-scaled truss structure.

Acknowledgements—The first author is grateful to Professor Fumio Nishino whose suggestion motivated him to investigate this problem. Thanks are due to Manabu Kobayashi and Keiichi Higuti for their assistance in numerical computations and figure drawings. The thorough reviews by the anonymous referees were helpful in revising this paper; Section 2 and Remarks 3.2, 3.4, 3.5 and 3.6 were added in reply to their comments.

REFERENCES

Conbescure, A. (1986). Static and dynamic buckling of large thin shells. *Nucl. Engng Des.* **92**, 339–354.
Elishakoff, I. (1988). Stochastic simulation of an initial imperfection data bank for isotropic shells with general imperfections. In *Buckling Structures* (Edited by I. Elishakoff *et al.*), pp. 195–209. Elsevier, Amsterdam.
Golubitsky, M. and Schaeffer, D. G. (1985). *Singularities and Groups in Bifurcation Theory*. Vol. 1, Springer, New York.
Hunt, G. W. (1977). Imperfection-sensitivity of semi-symmetric branching. *Proc. R. Soc.* **357**, 193–211.
Hutchinson, J. W. and Koiter, W. T. (1970). Postbuckling theory. *Appl. Mech. Rev.* **23**(12), 1353–1366.
Ikeda, K. and Murota, K. (1990). Computation of critical initial imperfection of truss structures. *J. Engng Mech. Div. ASCE* (to appear).
Iooss, G. and Joseph, D. D. (1981). *Elementary Stability and Bifurcation Theory*. Springer, New York.
Kam, T. Y. and Lee, F. S. (1986). Nonlinear analysis of steel plane frames with initial imperfections. *Comput. Struct.* **23**(4), 553–557.
Koiter, W. T. (1945). On the stability of elastic equilibrium. Dissertation. Delft, Holland (English translation: NASA Tech. Trans. F10: 833, 1967).
Lindberg, H. E. (1988). Random imperfections for dynamic pulse buckling. *J. Engng Mech. Div. ASCE* **114**(7), 1144–1165.
Murota, K. and Ikeda, K. (1990). Critical imperfection of axisymmetric structures. Tech. Rep. METR 90-03. Dept Math. Engng Info. Phys. Univ. Tokyo.
Nishino, F. and Hartono, W. (1989). Influential mode of imperfection on carrying capacity of structures. *J. Engng Mech. Div. ASCE.* **115**(10), 2150–2165.
Niwa, Y., Watanabe, E. and Nakagawa, N. (1981). Catastrophe and imperfection sensitivity of two-degree-of-freedom systems. *Proc. JSCE* **307**, 99–111.
Rosen, A. and Schmit, L. A., Jr. (1979). Design oriented analysis of imperfect truss structures—Part I—accurate analysis. *Int. J. Numer. Meth. Engng* **14**(9), 1309–1321.
Sattinger, D. H. (1979). *Group Theoretic Methods in Bifurcation Theory*. Lecture Notes in Mathematics, 762. Springer, New York.
Sattinger, D. H. (1980). Bifurcation and symmetry breaking in applied mathematics. *Bull. Am. Math. Soc.* **3**, 779–819.
Thompson, J. M. T. and Hunt, G. W. (1973). *A General Theory of Elastic Stability*. John Wiley, New York.
Van der Waerden, B. L. (1955). *Algebra*. Springer, New York.

APPENDIX

The solutions of eqns (30) are obtained in this Appendix for various kinds of simple critical points. Although $\bar{G}$ in eqn (27) may be expressed in terms of an infinite power series of w, it turns out to be sufficient for deriving the first-order approximation to consider up to the mth order terms of w for an mth order critical point. Then the mth order approximation to $\bar{G}$ is given by

$$\bar{G} \approx \bar{G}_m = \sum_{i=0}^{m} A_i w^i,$$

where

$$A_i = \sum_{j=0} \sum_{k=0} A_{ijk} \hat{f}^j \varepsilon^k.$$

Elimination of w from eqns (30) results in the condition that the discriminant of $\bar{G}_m$ (as a polynomial in w), or alternatively, the resultant of $\bar{G}_m$ and $\partial \bar{G}_m/\partial w$, should vanish. This condition can be written as (see, e.g. van der Waerden, 1955)

$$D_m = \begin{vmatrix} A_0 & A_1 & \cdot & \cdot & \cdot & \cdot & A_m & & \\ & A_0 & A_1 & \cdot & \cdot & \cdot & \cdot & A_m & \\ & & \cdot & \cdot & \cdot & \cdot & \cdot & \cdot & \\ & & & A_0 & A_1 & \cdot & \cdot & \cdot & A_m \\ A_1 & 2A_2 & \cdot & \cdot & mA_m & & & & \\ & A_1 & 2A_2 & \cdot & \cdot & mA_m & & & \\ & & \cdot & \cdot & \cdot & \cdot & & & \\ & & & A_1 & 2A_2 & \cdot & \cdot & mA_m & \end{vmatrix} \begin{matrix} \\ \\ \\ \\ \left.\begin{matrix} \\ \\ \\ \\ \end{matrix}\right\} m-1 \\ \left.\begin{matrix} \\ \\ \\ \\ \end{matrix}\right\} m \end{matrix} = 0. \tag{A1}$$

Note that D_m is a function in ε and $\hat{f}$, and that $\hat{f}$ is to be determined as a function in ε by the equation $D_m = 0$.

Limit point

For a non-degenerate limit point ($A_{010} \neq 0$, $A_{200} \neq 0$), the second-order approximation $\bar{G}_2$ of the bifurcation equation is employed:

$$\bar{G}_2 = A_0 + A_1 w + A_2 w^2,$$

in which

$$\begin{aligned} A_0 &= A_{001}\varepsilon + A_{010}\hat{f} + h.o.t.; \\ A_1 &= A_{101}\varepsilon + A_{110}\hat{f} + h.o.t.; \\ A_2 &= A_{200} + A_{201}\varepsilon + A_{210}\hat{f} + h.o.t. \end{aligned}$$

Then D_2 of eqn (A1) is evaluated to

$$D_2 = (4A_0A_2 - A_1^2)A_2 = 4(A_{001}\varepsilon + A_{010}\hat{f})A_{200}^2 + h.o.t.$$

Because $A_{010} \neq 0$ and $A_{200} \neq 0$, this equation yields

$$\hat{f}_c = \frac{-A_{001}}{A_{010}}\varepsilon + O(\varepsilon^2).$$

Simple asymmetric bifurcation point of order two

For a simple asymmetric bifurcation point of order two, for which $A_{010} = 0$ and $A_{200} \neq 0$, the condition (A1) with $m = 2$ becomes

$$D_2 = (4A_0A_2 - A_1^2)A_2 = 0. \tag{A2}$$

where

$$\begin{aligned} A_0 &= A_{001}\varepsilon + A_{020}\hat{f}^2 + A_{011}\hat{f}\varepsilon + h.o.t.; \\ A_1 &= A_{101}\varepsilon + A_{110}\hat{f} + h.o.t.; \\ A_2 &= A_{200} + h.o.t. \end{aligned} \tag{A3}$$

With the use of eqns (A3), (A2) becomes

$$\hat{f}_c^2 \approx \{4A_{200}A_{001}/(A_{110}^2 - 4A_{200}A_{020})\}\varepsilon, \tag{A4}$$

where the non-degeneracy condition $A_{110}^2 - 4A_{200}A_{020} > 0$ was employed. With reference to eqn (37) and this condition, eqn (A4) yields

$$\hat{f}_c \approx \pm\{4|A_{200}|A_{001}/(A_{110}^2 - 4A_{200}A_{020})\}^{1/2}\{\text{sign}\,(A_{200})\varepsilon\}^{1/2}.$$

Simple symmetric bifurcation point of order three

For a symmetric bifurcation point of order three, A_{300} is the first non-vanishing term of A_{m00} ($m = 1, 2, \ldots$). The condition (A1) with $m = 3$ is evaluated as

$$D_3 = (27A_0^2A_3^3 + 4A_1^3A_3^2) + (4A_0A_2^3A_3 - A_1^2A_2^2A_3 - 18A_0A_1A_2A_3^2) = 0, \tag{A5}$$

in which

$$\begin{aligned} A_0 &= A_{001}\varepsilon + A_{020}\hat{f}^2 + A_{011}\hat{f}\varepsilon + h.o.t.; \\ A_1 &= A_{101}\varepsilon + A_{110}\hat{f} + h.o.t.; \\ A_2 &= A_{201}\varepsilon + A_{210}\hat{f} + h.o.t.; \\ A_3 &= A_{300} + h.o.t. \end{aligned} \tag{A6}$$

Substituting (A6) into (A5) and noting that $A_{110} \neq 0$ (due to the non-degeneracy condition), we arrive at

$$\hat{f}_c \approx \frac{-3}{A_{110}} A_{300}^{1/3} \left| \frac{A_{001}}{2} \right|^{2/3} \varepsilon^{2/3}.$$

Simple bifurcation point of order greater than three

For a simple bifurcation point of order greater than three, it can be proved that

$$D_m = A_0^{m-1}(mA_m)^m - (-1)^m(m-1)^{m-1}A_1^m A_m^{m-1} + h.o.t.,$$

where

$$\begin{aligned} A_0 &= A_{001}\varepsilon + A_{020}\hat{f}^2 + h.o.t.; \\ A_1 &= A_{101}\varepsilon + A_{110}\hat{f} + h.o.t.; \\ A_m &= A_{m00} + h.o.t. \end{aligned}$$

Hence we have

$$\hat{f}_c = \frac{\pm m}{A_{110}} |A_{m00}|^{1/m} \left| \frac{A_{001}}{m-1} \right|^{1-1/m} \{\text{sign}\,(A_{m00})\varepsilon\}^{1-1/m}$$

for even m ($\geqslant 4$) and

$$\hat{f}_c \approx \frac{-m}{A_{110}} A_{m00}^{1/m} \left| \frac{A_{001}}{m-1} \right|^{1-1/m} \varepsilon^{1-1/m}$$

for odd m ($\geqslant 3$).